Proceedings of the ASME 27th International Conference on Offshore Mechanics and Arctic Engineering
OMAE2008
June 15-20, 2008, Estoril, Portugal

OMAE2008-57706

Predicting Spar VIM Using CFD

Samuel Holmes
Red Wing Engineering, Inc.

ABSTRACT

Recent work toward predicting spar vortex induced motion (VIM) with computational fluid dynamics (CFD) suggests that such simulations can anticipate many aspects of spar response and thus supplement tow tank experiments and other design methods. However, the results also highlight a number of challenges as well. The spar VIM problem is characterized by very high Reynolds numbers, geometric complexity including the presence of numerous external appendages and the presence of very rough surfaces. In this paper, we first review recent work on spar VIM where CFD was used to simulate tow tank experiments. This work suggests that CFD methods give good results in most cases but also points to some exceptions. In particular, in simulations of small scale vortex induced motion tests of spars, good agreement between analysis and experiments is usually obtained when the flow separates from the spar hull at the strakes. The CFD simulations are sometimes less successful at predicted VIM when flow separation occurs at the spar hull.

We then examine our own recent practice in simulating tow tank experiments with CFD with the objective of finding possible modeling deficiencies. The focus is on the resolution of the large eddies in the wake which most influence the fluctuating loads on the spar, but we are also concerned with the use of wall functions to model the boundary layer. All of the calculations use detached eddy simulation (DES). In order to test the method, we make use of wind tunnel experiments at on a fixed truncated cylinder without strakes. The wind tunnel experiments are performed at Reynolds numbers (Re) that are about the same as those used in scale model spar VIM experiments. Wake particle image velocimetry (PIV) and other data from wind tunnel experiments published in the open literature are used for comparison. The comparisons are used to examine requirements for grid resolution in the wake. Finally, it is suggested that specific wind tunnel experiments might be used to gather needed data on the effects of rough walls and appendages at very high Reynolds numbers.

BACKGROUND

Spars and other floating platforms are geometrically complex structures which are often festooned with external pipes, chains and anodes as shown in Figure 1. The wetted surfaces of a full scale spar are also typically rough although the model spars may be smooth. Typical tow tank tests of model spars are undertaken at Reynolds numbers on the order of 1e5 so a model spar with a smooth surface will probably have a laminar boundary layer up to the point of flow separation. A full scale spar may operate at Re in the tens of millions and will have a turbulent boundary layer before flow separation.

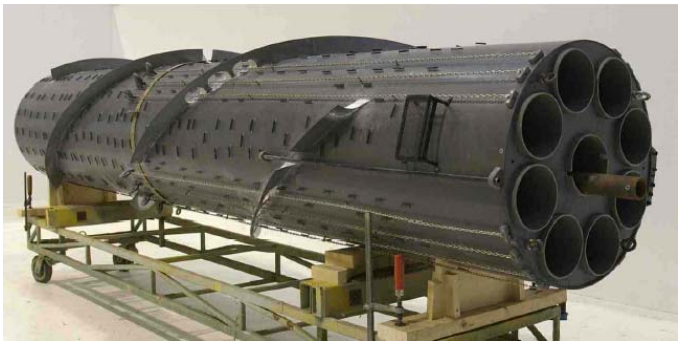

Figure 1. Model spar with external appendages

Simulating a spar in a tow tank or using CFD is made more complex by the spar's external appendages and by its surface roughness. Experimental data shows that these features have a significant affect on spar VIM. Oakley and Constantinides [1] reported an extensive series of experiments in which the number and arrangement of these appendages were varied. In the experiments, the inclusion or exclusion of external geometric details had a significant effect on VIM. They concluded that these features are necessary in tow tank experiments in order to get good results. Significantly, their experiments were conducted at Re greater than 1e6 so the boundary layer on the spar hull was turbulent at flow separation. In their accompanying CFD simulations, Oakley

and Constantinides [1] used a simplified modeling approach (also reported earlier in Reference 2) to keep the problem size reasonable. In essence, the small pipes and other features were modeled with a very coarse mesh relative to their diameter. Thus, the blocking effect of the appendages was modeled but the details of the flow around the appendages were not resolved.

In general, the comparisons of VIM amplitudes from analysis and from experiment reported by Oakley and Constainides are good with a few exceptions. However, the reasons for the disagreement between analysis and epxeriment are not understood and the overall data taken in the experiments does not reveal any details about the flow around the models. Other comparisons of CFD simulations with experiments have produced similar results. Halkyard et al. [3] and Atluri [4] reported a similar comparisons using experiments conducted at lower Re numbers (est. to be <1e5). Their experiments on a straked truss spar model showed a strong dependence of VIM on heading, i.e. at some most headings the spars showed an a/D[1] on the order of 0.05 or less but at some headings the VIM a/D went up to about 0.5. The increase in amplitude at some headings was attributed to the location of lines of flow separation. At most headings flow separated from the hull at the strakes but at some headings the flow separated along a line on the spar hull. I will suggest later in this paper that the errors in the CFD prediction of VIM amplitude in these later cases is due to errors in predicting the lines of separation on the hull.

In general, it is difficult to identify the source of errors in predicting VIM response to particular errors in flow prediction because the model tests usually don't include detailed flow measurements. Flow separation points, wake PIV data and pressures on the spar surface would be useful in assessing CFD effectiveness. This data is difficult to obtain in a tow tank experiment but might be more cheaply obtained in wind tunnel experiments remembering that for flow over a fixed object, the solution of the Navier-Stokes equations should be the same as long as the Reynolds number is the same in both cases. Because we are focused on CFD modeling issues, it is also thought that experiments on fixed structures (no VIM) would be almost as valuable as data from flexibly mounted structures. On the negative side, however, it should be kept in mind that the motion of a spar or spar model will tend to organize the wake into very large vortex structures which may not be present in a fixed spar at high Re. Thus the wake structures for the two cases are not likely to be the same.

One might consider an experiment in air in which the model is forced to move or is spring mounted and free to move. A problem in the latter case is the effect of the added mass of the surrounding fluid, which is significant in the case of tow tank test in water but negligible in a wind tunnel test. Finally, the flow speed in a wind tunnel test is typically two orders of magnitude greater than that in a tow tank test so the frequency of vortex shedding is proportionately greater. A 1 meter diameter model at a flow speed of 20m/s would have a shedding frequency of 4 Hz. A forced or free vibration of a model at this frequency in a wind tunnel seems possible but would present some design challenges.

In the remainder of this paper we look to wind tunnel data for comparison with our current modeling practice. Detailed flow measurement have been published by Pattenden et al. [5,6] on a truncated cylinder including wake PIV data, surface pressure measurements, lift and drag mean values and spectra. The data is not ideal because the cylinder has neither strakes nor appendages and its surface is smooth rather than rough. The smooth surface used in the wind tunnel experiments means the comparisons made here and any conclusions will only apply to small scale tow tank tests in which the model hull is also smooth. However, the data is taken at high Reynolds numbers from 1e5 to 2.5e5 or in the range of Re typical of tow tank experiments. The purpose of this comparison is to test our current modeling techniques and also to examine effects of mesh refinement in the wake and the boundary layer.

It should be noted that Pattenden not only performed the experiments used here for comparison but also completed extensive numerical studies. Pattenden performed calculations using large eddy simulation (LES), unsteady Reynolds averaged Navier Stokes (URANS) and detached eddy simulation (DES) turbulence models. In his simulations, which were similar in overall scale to those reported here, he obtained the best comparisons with the experimental data using LES.

NUMERICAL METHOD

All of the solutions shown here were produced using the AcuSolve™ finite element CFD solver. AcuSolve is based on the Galerkin/Least-Squares formulation and supports a variety of element types. AcuSolve uses a fully coupled pressure/velocity iterative solver plus a generalized alpha method as a semi-discrete time stepping algorithm. AcuSolve is second order accurate in space and time. The simulations also used Spalart's detached eddy simulation model (DES) [7, 8] to capture turbulence effects. In essence, the model treats the flow as a RANS calculation in the boundary layer and as an LES simulation elsewhere. It thus tends to be much more economical than a true LES simulation which requires a much finer mesh in the boundary layer.

Two meshes were created to model the flow over the cylinder. In the experiments. The first mesh is a "coarse" mesh of about 1M nodes and the second mesh is a "fine" mesh of about 8M nodes. The meshes are designed to model the wind tunnel experiments. Note that the model is large compared to the tunnel cross sectional area and the model is mounted on the floor of the tunnel so the floor boundary layer interacts with the cylinder. Both these features are included in the CFD simulations. Note that the floor boundary layer is not present in water with a free surface, but wind tunnel tests could be designed to eliminate this test feature. Figure 2 shows the overall geometry of the meshes while figure 3 shows the mesh detail for the coarse mesh. Both meshes are made up of tetrahedral elements with a side length on the order of 2mm or about 1/250 of the circumference of the cylinder at the surface. The coarse mesh gives an average y+ on the cylinder of 5 with

[1] a/D - vibration amplitude divided by spar diameter

a maximum of 10 while the fine mesh gave an average y+ at the surface of about 2. Both meshes used a courser grid to capture the boundary layer on the floor of the wind tunnel. In this area, the average y+ was on the order of 15 for the coarse mesh. The time step used with mesh 1 is 0.0003s and the time step used for mesh 2 is 0.00015s.

Finally, we used the built-in wall functions in AcuSolve™ in the solutions with the coarse mesh. These wall functions are designed to adjust for low values of y+ and for laminar and turbulent boundary layers. For calculations with the fine mesh, we used AcuSolve's low Reynolds number damping functions. A limited discussion of the implementation of wall functions can be found in [9]. We assumed that the cylinder is hydraulically smooth in all of the simulations.

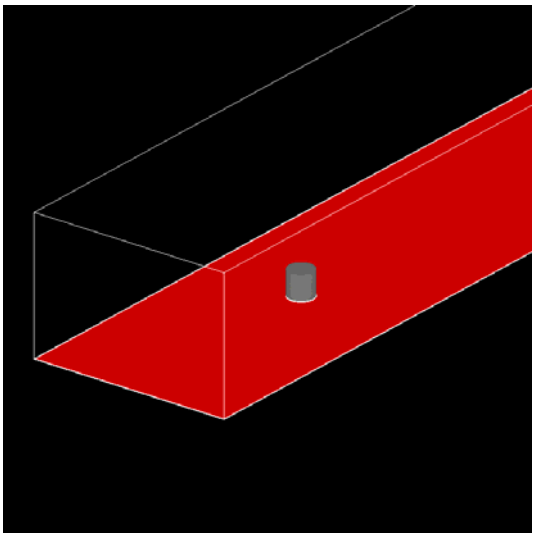

Figure 2. Overall mesh geometry

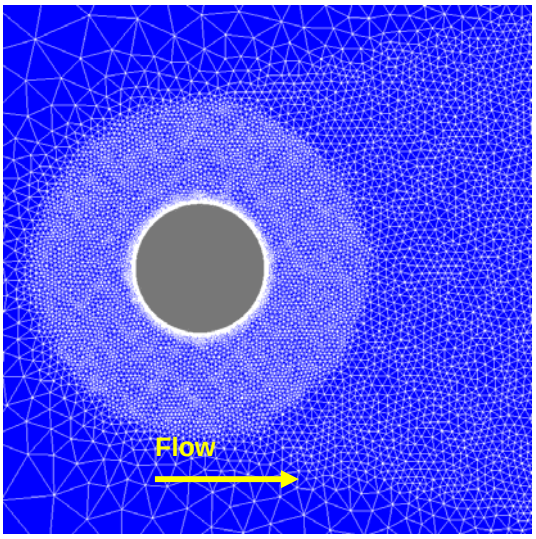

Figure 3. Mesh refinement around cylinder and in wake (coarse mesh)

COMPARISON WITH EXPERIMENTS

In [5] Pattenden reports experiments in which the wind tunnel free stream speed varied from 10m/s to 25m/s. He also gives wake PIV data at several points in the wake, lift and drag spectra data, pressure distributions around the cylinder at several heights and the velocity distribution in the boundary layer. I focused my simulations on speeds of 10m/s and 20m/s. Note that I will try to give a balanced view of the comparisons rather than show the best examples. In general, CFD simulations show reasonable agreement with the experimental data but also some important differences.

Figure 4 shows velocity vectors on a plane at the middle of the cylinder. The vectors are colored with velocity magnitude. The free stream speed is 20m/s in this case and the coarse mesh is being used. As shown, the flow separates from the cylinder at about 100 degrees and the wake shows fine vortex structures. A second view of the wake structure is shown in Figure 5 which shows contours of eddy viscosity. Note that the boundary layer is laminar as expected. Simulations using the fine mesh produced similar results.

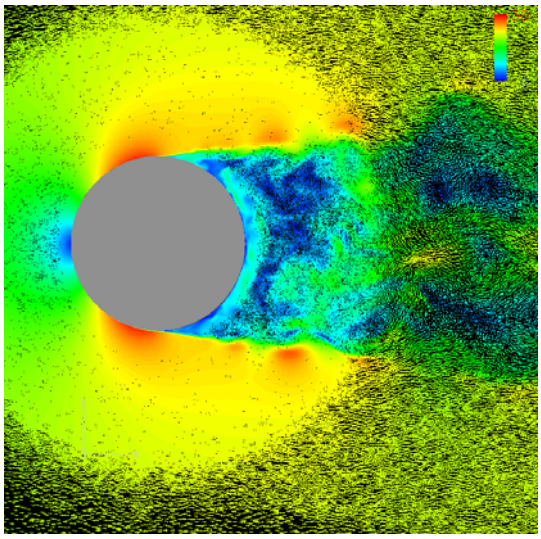

Figure 4. Velocity vectors colored with velocity magnitude

The pressure distribution around the cylinder is an important parameter in spar VIM studies and it is desired that lift and drag are accurately predicted. Figure 6 shows an example comparison of the measured pressure coefficient (Cp) around the cylinder at its mid-plane and the predicted values using the two meshes. As shown, the pressure is well resolved on the front surface of the cylinder but is not in very good agreement as we approach the 90-degree point or in the separated flow region. In particular, the experimental data suggests that flow separation occurs at about the 70-degree location while the analyses show separation much later at about the 90-degree location. Furthermore, the simulations over predict the pressure recovery in the wake. The net result is that drag is underestimated in the simulations. Most significantly, the two simulations are pretty similar; a significant increase in mesh resolution does not seem to help the accuracy at all. Table 1

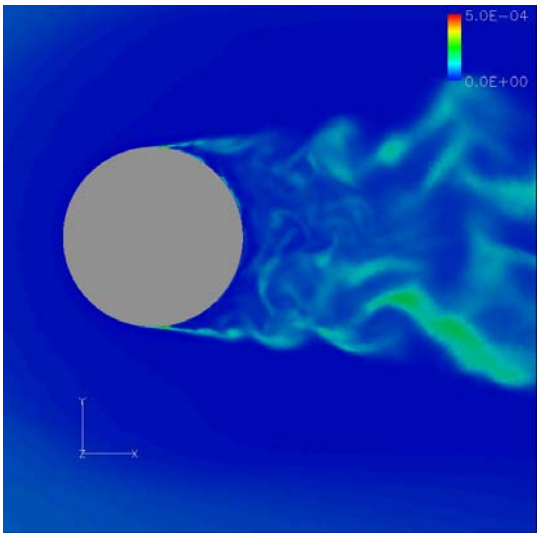

Figure 5. Contours of eddy viscosity

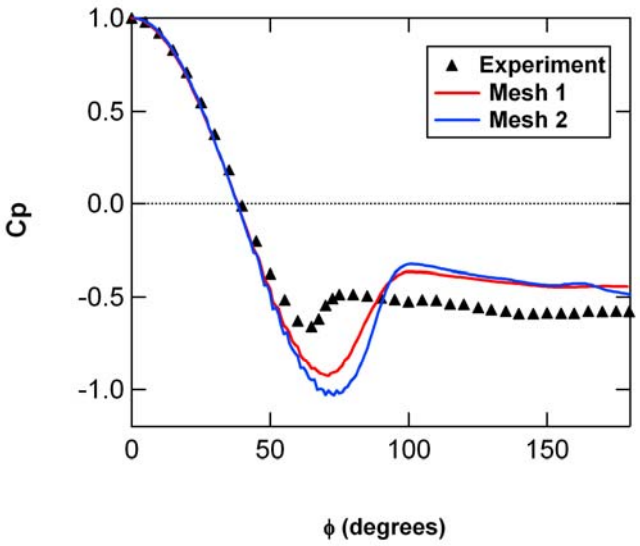

Figure 6. Comparison of time averaged pressure on cylinder surface at z = 0.075m.

Table 1. Measured and predicted overall drag coefficients

	Mesh 1	Mesh 2	Experiment
Cd (avg.)	0.68	0.66	0.79

compares the average drag coefficients from the experiments with those from the simulations. This error in predicting the line of separation may explain the errors in simulating spar tow tank tests discussed earlier. At those headings where the flow separates from the hull a delayed detachment of the flow might cause more curvature in the flow around the cylinder and hence more lift and an overestimation in displacement.

The simulation of spar motions is dependent on accurate resolution of the large vortex structures in the wake. A concern is that current practice might under-resolve these structures and thus produce errors. In DES simulations, it is assumed that the large anisotropic vortex structures are resolved and that the unresolved structures are isotropic. The effects of the unresolved structures are accounted for in the eddy viscosity which is calculated using Smagorinski's approximation [10]. The two meshes used here give a test of current modeling practice. The coarser mesh (mesh 1) is typical of many of the grids used in spar VIM studies. The average element size in the near wake in this grid is about 4 mm or about 1/40th of the model diamter. In experimental studies of turbulent flows over a wide range of scales it is found that the span from the largest unresolved eddies to the eddy size in which the turbulence appears isotropic is somewhat less than an order of magnitude. The largest eddies in the flow around a cylinder are usually on the order of the cylinder diameter so the smallest eddies that need to be resolved should be no less than 1/10th of the diameter (D). Assuming that it takes at least 5 nodal points of elements to capture an eddy one might expect that the maximum allowable element size in the near wake would be about 1/50 D or in our case about 3mm. Thus our coarse grid is close to this perceived limit.

In order to see how mesh resolution affects our solution in the wake, we examined the vortex structures predicted by the two grids by plotting the location and strength of vortex cores [11]. Figure 7 contrasts the vortex cores found at a single time steps using the coarse grid (top) and fine grid (bottom). As might be expected, the fine grid shows more fine vortex structure than the coarse grid. However, the larger vortex structures, most notably the axial structures in the shear layer next to the cylinder are similar in size, spacing and strength (as indicated by color). This suggests that the main features of the vortex structure are similar in both cases. Noting that the mesh refinement did not noticeably improve the solution results in other ways, we tentatively conclude that the resolution of the coarse mesh in the wake is adequate for this problem.

Examining the two vortex core structures in Figure 7 further we note that both show the large horseshoe shaped vortex around the cylinder at the ground plane although the fine mesh shows three parallel structures while the coarse mesh only shows one. We also see that the fine vortex structures resolved by the finer mesh are not generally oriented axially as are the larger structures. Thus a procession of eddies progressing toward an isotropic turbulence seems to be better presented in the latter case. In spite of this, the coarse mesh does an adequate job of predicted the flow with respect to the solution of the fine mesh if not to the experimental results.

Finally, we also take a look at the PIV measurements in the wake of the cylinder in Figure 8. Power spectra at a number of locations and under various flow conditions are presented in [5] and [6] but we only make one comparison here. This is at a flow speed of 20m/s and at a the location [0.15m ,0.15m ,0.15m] where the origin is on the centerline of the cylinder at

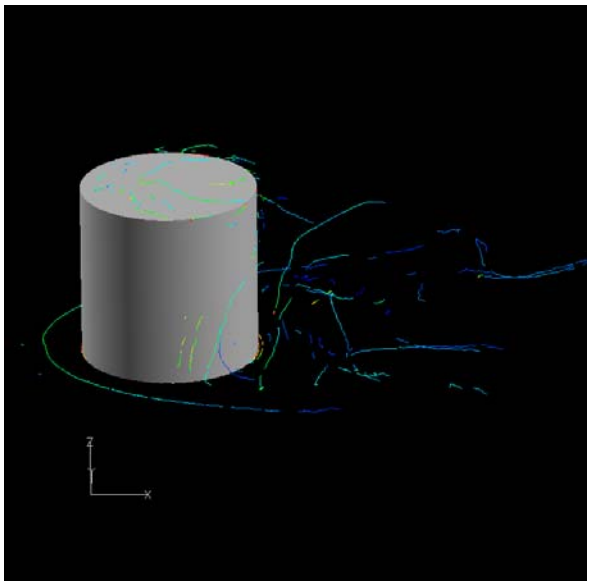

(a) Coarse Mesh

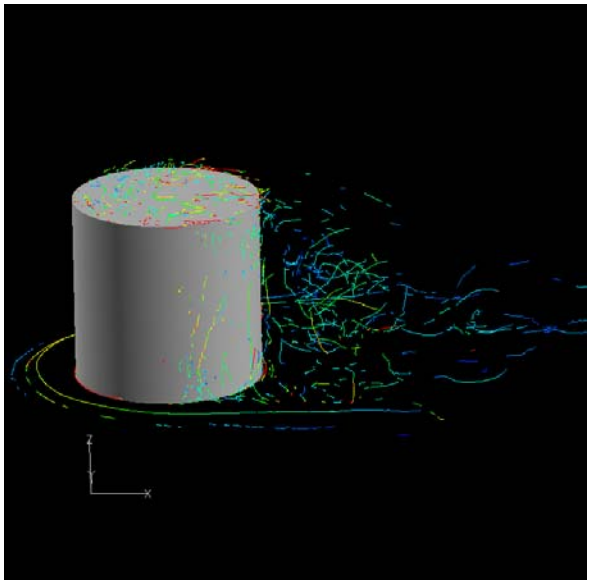

(b) Fine Mesh

Figure 7. Vortex cores

the floor level and the z-axis on the cylinder axis and positive upward. Thus the PIV data is taken in the shear layer near the top of the cylinder. In Figure 8 the experimental data is taken from [5] and the CFD data is taken from a sample of 8192 time steps. In processing this data, the sample window was divided into 4 shorter windows and the FFT and power spectrum of each subset calculated. The average values of the four resulting power spectra were then averaged to obtain a coarser but generally more reliable view of the power spectra (red and blue lines). As shown in the figure, the spectra from the CFD simulations show the same broad range of frequencies and about the same overall magnitude but do not model the peak in the experimental spectrum very well – missing the frequency at which this occurs. In this case, the fine mesh seems to over-predict the experimental data while the coarse mesh looks more similar in overall amplitude. This result is typical of the PIV data compared thus far although some show better and some show worse agreement than this particular case.

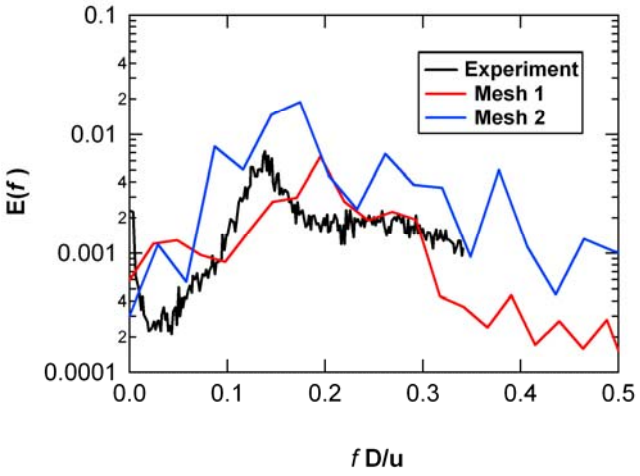

Figure 8. Power spectrum of U at x=1D, y=1D, z=1D at 20m/s inlet velocity

THE NEED FOR EXPERIMENTAL DATA

Recent experience suggests that, in general, CFD simulations can now capture many of the important aspects of spar VIM response at model tow tank scales or Reynolds numbers on the order of 1e5. However, some troubling problems remain. In particular, it seems that VIM is not well predicted when flow separation occurs at the spar hull. Also, the effect of appendages on separation is not well understood, but seemingly can be modeled. Collecting data on spars with these features at full scale Re of say 3e7 is much more difficult but may well be worth the effort. For example, it might be possible to collect boundary layer and separation data on an installed spar. However, collecting data in the wake seems to be an expensive proposition. An alternative to making measurements on a full scale spar might be to collect similar data in a wind tunnel. Large subsonic wind tunnels such as the subsonic NFAC 40 foot by 80 foot wind tunnel located at NASA-Ames in Mountain View could be used to collect PIV and other data at Re of about 12M (based on a flow speed of 50 m/s and a model diameter of about 4m). Such a model might include varying degrees of surface roughness and arrangements of external appendages.

SUMMARY & CONCLUSIONS

A comparison of CFD simulations with experimental data was undertaken using data from a wind tunnel test as a substitute for a towed bare spar. The modeling was done with a commercial solver using generally accepted practice for mesh generation, the use of turbulence model, wall functions, etc. Two meshes

were used, a coarse mesh of about 1M nodes that is typical of the resolution used in current practice to model spars in tow tank tests and a second mesh of 8M nodes representing a significant mesh refinement. It was found that both meshes gave fair overall agreement with the measured data, underestimating the drag but capturing other features of the flow. The errors in the Cd were attributed to errors predicting the line of separation of the flow and the pressure recovery in the wake. This is not uncommon in simulation on smooth cylinders. Other features of the flow were predicted with varying degrees of accuracy depending on the measurement location, etc. It is thought that this agreement will improve with larger sample sizes (longer runs). The results suggest that the current mesh size is adequate for many applications as the results did not improve noticeable with mesh refinement. It is suggested that the use of wind tunnels for selected geometries might offer an inexpensive means to improve existing modeling techniques.

ACKNOWLEDGEMENTS

The author would like to acknowledge the help of Dr. Stephen Turnock and Dr. Neil W. Bressloff of the University of Southampton who were kind enough to provide a copy of Dr. Richard John Pattenden's Thesis and electronic copies of data from some of the his experiments.

REFERENCES

1. Oakley, O. H., Constantinides, Y., "CFD Truss Spar Hull Benchmarking Study," OMAE2007-29150

2. Oakley, O. H., Constantinides, Y., Navarro, C. and Holmes, S. "Modeling Vortex Induced Motion of Spars in Uniform and Stratified Flows," OMAE2005-67238

3. Halkyard, J., Atluri, S. and Sirnivas, S. "Truss Spar Vortex Induced Motions: Benchmarking of CFD and Model Tests," OMAE2006-92673

4. Atluri, S., Halkyard, J. and Sirnivas, S. "CFD Simulation of Truss Spar Vortex Induced Motion," OMAE2006-92400

5. Pattenden, R. J., "An Investigation of the Flow Around a Truncated Cylinder," Ph.D. Thesis, University of Southhampton, (April 2004)

6. Pattenden, R. J.,Trunock, S. R. and Bressloff, N. W. "An Experimental and computational stiudy of the flow features found behind a truncated cylinder. 24th Symposium Naval Hydrodynamics, Jukuoka, Japan, July 2002

7. Spalart, P. R. and S. R. Allmaras, "A one-equation model for aerodynamic flows," AIAA 92-0439 (1992)

8. P. R. Spalart, S. Deck, M. L. Shur, K. D. Squires, M. Kh. Squires, and A. Travin, "A New Version of Detached Eddy Simulation, Resistant to Ambiguous Grid Densities," Submitted for publication in Theoretical and Computational Fluid Dynamics, 2005.

9. Ausolve Command Reference Manual, Version 1.7, Acusim Software Inc, (2007)

10. Smagorinsky, J. "General Circulation Experiments with the Primitive Equations," Part I, Mon. Wea. Res. 91, 99-152 (1958)

11. Sujudi, D. and Haimes, R. "Identification of Swirling Flow in 3D Vector Fields, AIAA 12th Computational Fluid Dynamics Conference, (1995)